0022-3565/05/3122-525–536$20.00
THE JOURNAL OF PHARMACOLOGY AND EXPERIMENTAL THERAPEUTICS
Copyright © 2005 by The American Society for Pharmacology and Experimental Therapeutics
JPET 312:525–536, 2005

Vol. 312, No. 2
74195/1193241
Printed in U.S.A.

5-aza-Cytidine Is a Potent Inhibitor of DNA Methyltransferase 3a and Induces Apoptosis in HCT-116 Colon Cancer Cells via Gadd45- and p53-Dependent Mechanisms

Regine Schneider-Stock, Mona Diab-Assef, Astrid Ro[illegible]ck, Charlotte Foltze[illegible]urd[illegible]e, Carsten Boltze, Roland Hartig, Peter Schönfeld, A[illegible]ert H[illegible]ssner, and Hala G[illegible]li-[illegible]htas[illegible]

Departments of Pathology (R.S.S., A.R., C.B., A.R.), Immunology [illegible] and Biochem[illegible] (P.S.), [illegible]-Guericke [illegible]versity, Magdeburg, Germany; Department of Biology, American Universi[illegible] of Be[illegible] Beirut, Lebanon (H[illegible].M., H[illegible].A.); and Institut National de la Santé et de la Recherche Médicale, Strasbour[illegible] France (C.[illegible]

Received July 13, 2004; accepted November 9, 2004

ABSTRACT

Methyltransferase inhibitors commonly used [illegible]s promote tumor cell death, but their detailed cyto[illegible]ic a[illegible] not yet fully understood. A deeper knowledge abo[illegible] th[illegible] apoptosis-inducing mechanisms and th[illegible]raction[illegible]h DNA methyltransferases (DNMTs) DNM[illegible], DN[illegible]3a, and [illegible]NMT3b might allow the design of m[illegible] effecti[illegible] drugs w[illegible] lower cytotoxicity. 5-aza-cytidine (5-a[illegible]CR), [illegible]hibitor of DNMT1, is known to indu[illegible]eme[illegible]on and reactivation of silenced genes. In this s[illegible], we inv[illegible]ated the p53 dependence of apoptotic, c[illegible]y[illegible] and grow[illegible]hibitory effects of 5-aza-CR, as well [illegible]s the in[illegible]ce on the expression level of DNMT1, DNMT3[illegible]and DNMT[illegible] the colon cancer c[illegible]e HCT-116. Ex[illegible]ure to 5-aza-C[illegible]duced the up-regula[illegible] of genes pr[illegible]oting c[illegible]cycle arrest and DNA repai[illegible]^{21WA} and GADD4[illegible] a[illegible]tosis (p53, RIPK2, Bak1, c[illegible]pas[illegible] and caspase 6). In parallel, there[illegible] down-regulation of anti-apoptotic P[illegible]tein and t[illegible]$_2$/M-mediator cyclin B1. Coincubation w[illegible]fithrin-alpha (PFT-α), a selective p53 inhibitor, restored GAD[illegible]Bcl2, cyclin B1, and p21^{WAF1} expression levels a[illegible]almost[illegible]tely reversed the growth inhibitory, cell c[illegible]e, and apop[illegible] effects of 5-aza-CR. 5-aza-CR treatme[illegible]caus[illegible]al demethylation and reactivation of p16^{INK4} exp[illegible] Th[illegible] was a marked decrease in DNMT1 and DNMT3a mR[illegible] expression, with PFT-α reversing these effects. Ho[illegible], 5-aza-CR treatment did not modulate DNMT3b e[illegible]ssion. Our data demonstrate that 5-aza-CR action in HC[illegible]6 is mediated by p53 and its downstream effectors p21[illegible] and GADD45. This is the first report to show a link [illegible]een p53 and regulation of DNMT1 and de novo methyltransferase DNMT3a.

Si[illegible]he causal relationship be[illegible]n hype[illegible]thylation of the pro[illegible]r of tumo[illegible]ressor ge[illegible]nd [illegible]e development of cancer [illegible]as been c[illegible]y[illegible]astrat[illegible]ecific demethylating agents are of i[illegible]est [illegible]in molecular targeted therapeutics (Zhu and [illegible]ten[illegible], 20[illegible]). Methylation of cytosines within CpG din[illegible]ides is associated with transcription[illegible]silencing dur[illegible] mammalian development and tumorig[illegible] (Bird, 1996). [illegible]e main enzyme responsible for replicati[illegible] th[illegible]NA methy[illegible]tion pattern is the DNA meth[illegible]sfe[illegible]ase (D[illegible]T) 1. In contrast, DNMT3a and DMMT3b are [illegible]sponsible fo[illegible]novo methylation, in which a methyl-grou[illegible]nsferred to the carbon position of the cytosine from the [illegible]hyl donor *S*-adenosyl-L-methionine (Okano et al., 1999).

To date, 5-aza-cytidine (5-aza-CR) and its deoxyribose analog 5-aza-2′-deoxycytidine are the DNMT inhibitors that have undergone the most preclinical and clinical testing (Santini et al., 2001). 5-aza-CR was evaluated in clinical trials as a cancer therapeutic agent for the treatment of patients with acute myeloid leukemia and myelodysplastic syndrome (Santini et al., 2001; Kornblith et al., 2002; Silverman et al., 2002). 5-aza-CR incorporates into DNA forming covalent adducts with cellular DNMT1, thereby depleting the cells from enzyme activity and causing demethylation of genomic DNA as a secondary consequence (Christman, 2002). In various in vitro experiments, 5-aza-CR treatment leads to re-expression of former silenced genes (Christman, 2002). The resulting DNA hypomethylation has been linked to the induction of cellular differentiation in vitro (Petti et al., 1993) and altered expression of genes involved in tumor suppression (Christman, 2002). In addition, it has been dem-

Art[illegible] publication date, and citation information can be found at http://jpet.aspetjournals.org.
doi:10.1124/jpet.104.074195.

ABBREVIATIONS: DNMT, DNA methyltransferase; 5-aza-CR, 5-aza-cytidine; PFT-α, pifithrin-α; PI, propidium iodide; PCR, polymerase chain reaction; [^{3}H]SAM, *S*-adenosyl-L-[methyl-^{3}H]methionine; MTT, 3-(4,5-dimethylthiazol-2-yl)-2,5-diphenyltetrazolium; PBS, phosphate-buffered saline; TUNEL, terminal deoxyribonucleotidyl transferase-mediated dUTP nick-end labeling; FITC, fluorescein isothiocyanate; β2-M, β2-microglobulin.

onstrated that 5-aza-CR inhibits telomerase activity via transcriptional repression of hTERT in prostate cancer cell lines (Kitagawa et al., 2000). Recent studies have demonstrated that DNMT1-5-aza-2′-deoxycytidine adducts in DNA can activate a p53 DNA damage response pathway in the colon cancer cell line HCT-116 (Karpf et al., 2001, 2004). However, the mechanism responsible for this drug's inhibition of cell growth and its other biological effects remain unclear.

In the present study, we examined the effects of 5-aza-CR on apoptosis, cell growth, global methylation status, and the expression of the methyltransferases DNMT1, DNMT3a, and DNMT3b in the human colon cancer cell line HCT-116. To develop a mechanistic model of 5-aza-CR action, we investigated the observed effects before and after treatment with the selective p53 inhibitor, pifithrin-α (PFT-α), as well as in HCT (−/− p53) cells. We found a possible link between p53 and the regulation of methyltransferases after 5-aza treatment.

Materials and Methods

Reagents and Drugs. Prolong Antifade and [illegible]iodide (PI) were purchased from Molecular Probes (Eugene, OR). [illegible] and trypan blue were obtained from Sigma-Aldrich ([illegible] Louis, MO). RPMI 1640, fetal bovine serum, and penicillin-streptomycin were obtained from Invitrogen (Carlsbad, CA).

Methylation-Specific PCR. Genomic DNA was prepared using the standard proteinase K-phenol-chloroform extraction method. The methylation status of the p16 gene was determined by methylation-specific PCR. Bisulfite modification was performed using the CpGenome modification kit (Chemicon Intergene, Carlsbad, CA). Two microliters of bisulfite-modified DNA was amplified by PCR, using primers that were specific for methylated or unmethylated sequences of p16^{INK4a} gene as described previously (Schneider-Stock et al., 2003). PCR amplified products were separated by electrophoresis on 8% polyacrylamide gels and visualized by silver staining.

Global Genomic DNA Methylation Status. The methylation status of CpG islands in genomic DNA was determined by the in vitro methylation capacity of DNA by using *S*-adenosyl-L-methyl-[^{3}H]methionine ([^{3}H]SAM; Amersham Biosciences, Piscataway, NJ) as methyl donor and a prokaryotic CpG DNA methyltransferase (SssI methylase; New England Biolabs, Beverly, MA). The manner in which this assay is performed provides a reciprocal relationship between the endogenous DNA methylation status and the exogenous methyl-^{3}H-methyl incorporation. Briefly, 2 μg genomic DNA was digested to completion overnight with EcoRI (10 U/μg of DNA) according to the recommendations of the manufacturer (AGS, Heidelberg, Germany). Digested DNA (1 μg) was incubated, in triplicate, in 25 μl containing 2 U of SssI methylase, 2 μM [^{3}H]SAM, and 2 μM nonradioactive SAM (New England Biolabs) in the buffer supplied by the manufacturer. The reaction mixture was incubated at 37°C for 2 h. The reaction was stopped by heating at 65°C for 10 min. Reaction mixtures not containing enzyme were used as background controls for each DNA sample. The incubation mixtures were applied onto 2.5-cm Whatman DE-81 ion exchange filters (Fisher Scientific Co., Pittsburgh, PA) by using a vacuum filtration apparatus; the disks were then washed with 0.35 M Na_2HPO_4 for 45 min. The disks were dried at 55°C for 30 min, and the resulting radioactivity of the DNA bound on the disks was measured by scintillation counting with Tri-Carb Liquid Scintillation Analyzer 2100 TR (PerkinElmer Life and Analytical Sciences, Boston, MA).

Cell Growth and Treatment. The human colon cancer cells HCT-116 (+/+ and −/− p53) were cultured in RPMI 1640 medium. Cells were grown at 37°C in an atmosphere of 5% CO_2 supplemented with penicillin (100 U/ml), streptomycin (100 mg/ml), and 10% fetal calf serum. For experiments, cells seeded on six-well plates at a density of 4×10^4 cells per well, were left to grow. 3-(4,5-Dimethylthiazol-2-yl)-2,5-diphenyltetrazolium (MTT) (Calbiochem, San Diego, CA) reduction by cells was used to assess drug-induced cell growth inhibition and cytotoxicity. The proliferation assay used was a MTT-based method to measure the ability of metabolically active cells converting tetrazolium [illegible] a cleavage product. The absorbance was recorded at [illegible] nm. Cell proliferation and cytotoxicity were determined using the Cell Titer [illegible] nonradioactive cell proliferation assay (Sigma-Tau[illegible]hen, Germany) according to the manufacturer's suggestions.

Treatment. Cells were treated with 1 or 5 μM of freshly prepared 5-aza-CR (Sigma-Aldrich) 24 h after plating and treatment was replenished [illegible]. Assays were conducted after exposure harvested 1, 2, and 4 days after treatment. [illegible] of cells with the active p53 inhibitor PFT-α, was performed by pretreating the cells with the inhibitor prior to addition of 5-aza-CR.

To determine whether cells recover from 5-aza-CR treatment, cells were replenished with fresh medium without drug at 96 h post-treatment and were allowed to recover for a further 48 h (total of 144 h).

Flow Cytometric Analysis of DNA Content. Cells were seeded in 10-cm dishes at a density of 5×10^5 cells per well. They were incubated and allowed to grow to 40% confluence after which they were treated with 1 μM 5-aza-CR and incubated for further 72 h. They were then harvested by trypsin release, washed twice with phosphate-buffered saline (PBS), permeabilized with 70% ethanol, treated with 1% RNase, and finally stained with propidium iodide solution (10 μg/ml final concentration). Distribution of cell cycle phases with different DNA contents was determined using a flow cytometer (FACSCalibur (BD Biosciences, San Jose, CA). Cells less intense stained than G_1 cells (sub G_1 cells) in flow cytometric histograms were considered as apoptotic cells and cell debris. Analysis of cell cycle distribution and the percentage of cells in the G_1, S, and G_2 phases of the cell cycle were determined using Cell QuestPro and ModFitLT (Verity Software House, Topsham, ME) software.

Apoptosis: Terminal Deoxyribonucleotidyl Transferase (TdT)-Mediated dUTP Nick-End Labeling (TUNEL) and Annexin V Assays. *TUNEL assay.* Apoptosis was scored either by assessing the fraction of cells with a sub-G_0/G_1 DNA content by flow cytometry (see above) or by estimating the extent of DNA fragmentation using the TUNEL assay. Briefly, cells were plated on autoclaved glass coverslips in six-well culture plates and treated with 1 μM 5-aza-CR or PFT-α as described earlier. The medium was then aspirated and cells were washed twice with warm PBS. Cellular DNA was stained with the In Situ Cell Death Detection kit (Roche Diagnostics, Mannheim, Germany), and the assay was performed according to the recommendations of the manufacturer (Roche Diagnostics). Cytospin preparations were fixed and labeled and four independent ×100 fields containing a minimum of 300 cells on each of three replicate slides were evaluated for nuclear labeling by fluorescence microscopy (Axiovert 200; Carl Zeiss GmbH, Jena, Germany) for each treatment. Nuclear chromatin condensation was observed by fluorescence microscopy (LSM 410, Carl Zeiss GmbH, Germany).

Annexin-V-FITC binding assay. After exposure to 10 μM 5-aza-CR for 6 h, cells were washed twice with cold PBS. Binding to annexin V-FITC to the cell surface, which is an early marker of apoptosis, was determined according to the instruction of the manufacturer (BD Biosciences PharMingen, San Diego, CA). The slides were viewed immediately on a fluorescence microscope [Leica DMRE7 (Leica, Wetzlar, Germany) equipped with a SpotRT camera (Diagnostics Instruments, Burroughs, MI)]. Images were captured and pseudocolored using Spot camera Software. For each of the three replicate experiments, three randomly selected microscopic fields were examined at 400× magnification, and the annexin V-FITC cells (green fluorescence) were counted.

Real-Time RT-PCR for Detection of mRNA Expression. For mRNA expression studies, total RNA was extracted using TRIzol reagent (Invitrogen). cDNA synthesis was done in a 20-μl reaction mix starting with 1 μg of total RNA using the reverse transcription system of Promega (Madison, WI; 42°C for 30 min, 99°C for 5 min, and 4°C for 5 min). Real-time PCR was performed using a LightCycler (Roche Diagnostics), and threshold cycle numbers were determined using the LightCycler software, version 3.5. Each sample was run twice, and the threshold cycle numbers were averaged. In addition, all samples showing >10% deviation of their values were tested in a third run. For amplicon detection, the LightCycler DNA Master Hybridization Probes Kit was used as described by the manufacturer (Roche Diagnostics). Briefly, in addition to the two primers, two different oligonucleotides hybridize each to internal sequence of the experimental genes or the β2-microglobulin (β2-M) gene. PCR assays were carried out in a 20-μl reaction volume containing 1 μl of cDNAs, 0.5 μM of each primer, 2 pmol LCRed 640 probe, 4 pmol fluorescein hybridization probe, and 2.5 mM $MgCl_2$. Annealing temperatures are given in Table 1. All genes examined were normalized to housekeeping gene encoding β2-M.

-Fold induction was calculated according to the formula $2^{(Rt-Et)}/2^{(Rn-En)}$ (Saha et al., 2001), where *Rt* is the threshold cycle number for the β2-M gene observed in the cell line after 5-aza-CR treatment, *Et* is the threshold cycle number for the experimental gene observed in cell line after 5-aza-CR-treatment, *Rn* is the threshold cycle number for the β2-M gene observed in the cell line before 5-aza-CR treatment, and *En* is the threshold cycle number for the experimental gene observed in the cell line before 5-aza-CR-treatment. Primers and oligonucleotide probes were chosen using the TIB MOLBIOL LightCycler primer program (Berlin, Germany; http://www.tibmolbiol.de/kitagoag.html) to ensure their total gene specificity (Table 1). Primer sequences for p53, Bcl-2, $p21^{WAF1}$, and β 2-M have been previously described (Chen et al., 2004). Primers for DNMT1, DNMT3a, DNMT3b, GADD45, and $p16^{INK4a}$ are summarized in Table 1.

Protein Extraction and Quantification. Cell samples were homogenized in a buffer at pH 7.5 containing 50 mM sodium phosphate, 0.2 M NaCl, 1 mM EDTA, 10 μM E-64, and 1 mM phenylmethylsulfonyl fluoride by sonication (Sonifier, Bandelin, Berlin, Germany). Homogenates were centrifuged for 10 min at 4°C at 10,000 rpm (Eppendorf, Hamburg, Germany). The supernatant was stored in three aliquots at −20°C or immediately reduced by adding 5× Laemmli buffer containing 20% dithiothreitol and boiled. Protein measurements were carried out in all samples according to the Bio-Rad DC Protein Assay (Bio-Rad, Hercules, Ca), and equal protein amounts were subjected to SDS-PAGE followed by immunoblotting.

Western Blotting. After transferring to a polyvinylidene difluoride membrane (PerkinElmer Life and Analytical Sciences, Boston, MA) and blocking nonspecific binding with 5% milk, it was incubated with the specific antibodies followed by incubation with the secondary peroxidase conjugated goat anti-rabbit antibody (1:30,000) for 30 min. We used the following human reactive monoclonal or polyclonal antibodies: anti-$p21^{WAF1}$ (clone EA10, Oncogene Science, Cambridge, MA), anti-p53 (clone DO-1, Oncogene Science), anti-DNMT1 (Dako Corporation, Denmark A/S, Glostrup, Denmark), anti-DNMT3a (clone 64B1446; Biocarta), and DNMT3b (clone 2A 1018, Biocarta). β-Actin antibody (clone HUM-1) was purchased from Novocastra. The substrate, West Pico Chemiluminescence (Pierce Chemical, Rockford, IL), was left on the membrane until distinct bands had developed (maximum 30 min). The ECL membrane images were evaluated for the identification of the protein expression, using the GeneGnome and GeneTools image scanning and analysis package (Syngene Bio-Imaging Systems; Synoptics Inc., Frederick, MD). Hybridization with the housekeeping protein β-actin was used as a control of equal loading and protein quality.

cDNA Array Analysis. To identify apoptosis-associated genes that are regulated by 5-aza-CR, we used GEArray Q series Human Apoptosis Gene Array designed to profile the expression of 96 key genes involved in apoptosis (Superarray Bioscience Corp., Bethesda, MD). The complete gene list can be found at http://www.superarray.com. The cDNA fragments are printed on a 3.8- × 4.8-cm nylon membrane. Total RNA was prepared by TRIzol Reagent (Invitrogen). An aliquot of 4 μg of total RNA was reversely transcribed (Promega), and the probe was simultaneously labeled using the GEA labeling buffer mix (Biotin-16-dUTP; Roche Diagnostics) according to the instructions of the manufacturer. The membrane was prehybridized with sheared salmon sperm DNA in GEAhyb Hybridization

TABLE 1

Sequences of primers, hybridization probes, annealing temperatures, and lengths of PCR products

DNMT1	332-bp product	XM_017218[a]	62°C
DNMT 1 S	5′-CT TCT ATC TCC TC CCT A		
DNMT 1 A	5′-gCA gT TgTgAACACTgTg		
hyb DNMT1 LC	5′-Red640- Tgg gCC ATC gAg Atg Tgg gAC p		
hyb DNMT1 FL	5′-TT A gCA ggC ATC TCT gAC AC X		
DNMT3a	191-bp product	AF_067972	62°C
Met 3a F 1	CA CAg AAg CAT ATC CAg gAg Tg		
Met 3a R 1	-gT TC ACT TTg CTg AAC TTg GC		
hyb DNMT3a FL	5′-ACg Atg gAg Agg TCA TTg CAg ggA C X		
hyb DNMT3a LC	5′-LC Red640-gCC CCC AAT CAC CAg ATC gAA Tg p		
DNMT3b	191-bp product	XM_009449	62°C
M 3b	5′-AAT gTg AAT CCA gCC Agg AAA ggC		
M 3b-	5′-ACT ggA TTA CAC TCC Agg AAC CgT		
hyb DNMT L	5′-ggC gTg AgT AAT TCA gCA ggT ggT X		
hyb DNMT3	5′-LC Red640-ATT CgA AgA AgA gCC ggC CTg TAC C p		
GADD45	212-bp product	NM_001924	57°C
GA 5F	5′-CTg CgT gCT ggT gAC gAA		
GAD A	5′-Agg gAg TAA CTg CTT gAg TAG CTA		
hyb DD45 FL	5′-TCA ggg AgA TTA ATC ACT ggA ACC C X		
hyb DD45 LC	5′-LC Red640-TTG ATC CAT gTA gCg ACT TTC CCg-PH		
p16	127-bp product	NM_000077	63°C
P16 F	5′-Tgg ACC Tgg CTg Agg AgC T		
P16 A	5′-TCA ATC ggg gAT gTC TgA g		
hyb p16 FL	5′-gCg gCA TCT Atg Cgg gCA Tgg TT X		
hyb p16 LC	5′-LC Red640-CTg CCT CTg gTg CCC CCC gC p		

LC, LightCycler Red 640; X, fluorescein; p, phosphate; hyb, hybridization probe.
[a] GenBank accession number.

Solution followed by hybridization at 68°C overnight with continuous agitation. The membrane was washed at 68°C twice with 2× standard saline citrate, 1% SDS and 0.1× standard saline citrate, 0.5% SDS, respectively. For detection of chemiluminescence, the membrane was blocked using the alkaline phosphatase-conjugated streptavidin method in combination with CPD star. All signals were measured using the Syngene BIO Imaging system. The raw signal intensities were corrected for background by subtracting the signal intensity of the average of the three negative controls (pUC18 cDNA) and the four blanks and were expressed as -fold changes given as the relative expression ratio: gene/housekeeping gene. Any signal whose raw intensity was less than 150% of the background was treated as a background signal and thus interpreted to be not detectable in the sample.

Results

5-aza-CR Induces Demethylation and Significant Down-Regulation of DNMT1 and DNMT3a Gene Transcription in HCT-116 Cells. We determined the time-course effects of 5-aza-CR on the level of global DNA methylation in p53 (+/+) HCT-116 cells by incubating DNA with [^{3}H]SAM in the presence of bacterial SssI methylase. In this assay, the number of methyl groups incorporated into DNA in the presence of [^{3}H]SAM and SssI methylase is inversely proportional to the original number of CpG sites available for methylation. Thus, it is inversely proportional to the prior methylation status of DNA. The DNA isolated from HCT-116 cells treated with 1 μM 5-aza-CR was significantly hypomethylated after 72 ($p < 0.05$) and 96 ($p < 0.01$) of treatment compared with cells not treated with the drug, indicating that 5-aza-CR decreased the global level of DNA methylation in a time-dependent manner (Fig. 1A). Considering the fact that hemimethylation of the p16^{INK4a} promotor is observed in HCT-116 cells (presence of both methylated and unmethylated bands in the untreated control), we assessed the effect of 5-aza-CR on the methylation status of the p16^{INK4a} gene promoter following treatment with 5-aza-CR (1 μM) for 3 days, methylated band almost completely disappeared after 96 h (Fig. 1B). Corresponding to the disappearance of the methylation-specific band was the dependent re-expression of p16^{INK4a} mRNA in HCT-116 cells (Fig. 1C). Up-regulation of p16^{INK4a} transcripts occurred when cells were allowed to recover from 5-aza-CR treatment.

When determining the effect of 5-aza-CR on the expression of human DNMT1, DNMT3a, and DNMT3b. Real-time PCR revealed a 3-fold down-regulation of DNMT1 mRNA expression levels following treatment with 5-aza-CR for 4 days (Fig. 1D). A significant down-regulation in DNMT3a expression levels occurred as early as 24 h post-treatment, peaking at 48 h, and persisted even after 4 days of treatment with 5-aza-CR (Fig. 1E). Consistent 5-aza-CR treatment did not affect the mRNA expression levels of DNMT3b (Fig. 1F).

5-aza-CR Treatment Induces Growth Inhibition and G$_2$/M Arrest in HCT-116 Cells. The time of exposure to 5-aza-CR required to inhibit cell growth was evaluated in p53 (+/+) HCT-116 cells. Cells were treated with 5-aza-CR and cell morphology and viability were monitored for 96 h by the MTT assay. The addition of 5-aza-CR resulted

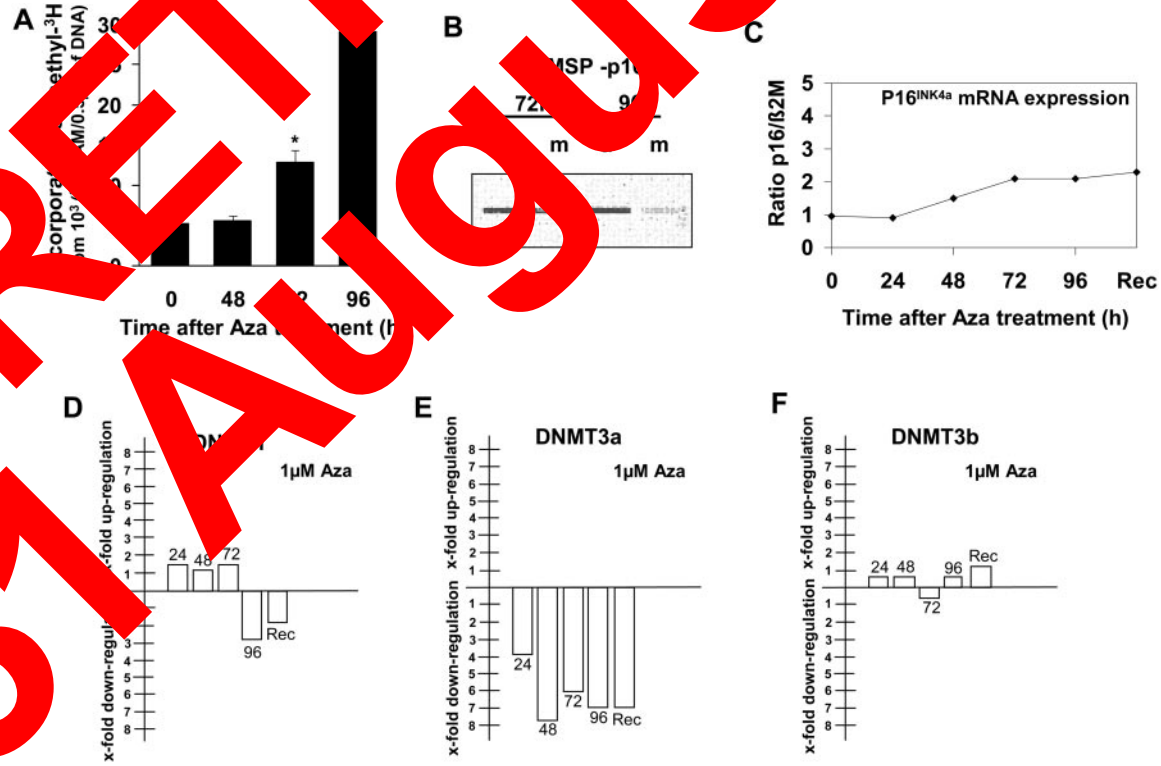

Fig. 1. A, time-course analysis of the global DNA methylation status in HCT-116 (p53 +/+) cells cultured in the presence of 0 or 1 μM 5-aza-CR. The extent of global DNA methylation is inversely proportional to the incorporation of methyl groups by bacterial SssI methylase in the presence of [^{3}H]SAM. Values are means ± S.E.M., $n = 3$. ANOVA, Aza, 72 h, $p < 0.001$; Aza, 96 h, $p < 0.006$. B, effect of 5-aza-CR on p16^{INK4a} gene methylation. Methylation-specific PCR was performed using the unmethylated (u) and methylated (m) primer sets. C, time-course analysis of mRNA re-expression of p16^{INK4a}. D to F, expression of the DNA methyltransferases DNMT1, DNMT3a, and DNMT3b in HCT-116 cells cultured in the presence of 1 μM 5-aza-CR.

in the appearance of many damaged cells at 72 h after treatment and to a lesser extent at 48 h (Fig. 2A). A time-dependent inhibition of cell viability was observed upon treatment with 5-aza-CR; 1 μM decreased cell viability by 65% at 72 h post-treatment (Fig. 2A). At 96 h, the viability of HCT-116 cells was most severely affected presumably because growth inhibition requires both the incorporation of 5-aza-CR into genomic DNA and time for the alteration of DNA methylation patterns and the accumulation of enzyme DNA adducts. In addition, the kinetics of the induction of methylation-silenced genes (Fig. 1C) and cell growth inhibition after 5-aza-CR was consistent with this time frame of treatment.

To dissect the mechanism of the antiproliferative effects of 5-aza-CR, we determined whether growth inhibition is associated with specific cell cycle changes. Exponentially growing HCT-116 (+/+) cells were treated with 5-aza-CR for 48 or 72 h and harvested for flow cytometric analysis of DNA content by PI staining (Fig. 2B). Cell cycle distribution a[n]ysis showed an increase, within 48 h, in the number o[f] cells in the G_2 phase of the cell cycle following treatment [w]ith 1 μM 5-aza-CR, providing evidence of G_2/M arrest. By [7]2 h, 50% of the cells arrested at G_2 phase, and the [p]ercenta[g]e of cells in S phase decreased by more than 50% [a]s com[p]ared with the untreated control. Furthermore, [t]he ac[t] of 5-aza-CR for 72 h induced an accumulation [o]f sub-G_0-G_1 (apoptotic) DNA. Thus, the growth inhibitory effects of 5-aza-CR (Fig. 2A) are due to induction of G_2/M arrest and programmed cell death (Fig. 2B).

5-aza-CR Induces Apoptosis in HCT-116 Cells. To understand and confirm the nature of cell death, we used the TUNEL and Annexin-V flow cytometric assay methods (Fig. 3). Numerous TUNEL-positive cells with apoptotic characteristics, based on the [c]ondensed shrunken shape of the nucleus and on intense staining of [F]ITC-conjugated dUTP, appeared in the 5-aza-[C]R-treated c[u]ltures (Fig. [3], left). A time-dependent increase of up to [2]% in apoptotic cells occurred in 5-aza-CR-treated cultures (Fig. 3A, [r]ight). Drug exposure also caused a strong increase in annexin-V staining, a typical feature of early apoptosis (Fig. 3B, [r]ight). The promotion of apoptotic cells at 72 h post-treatment was significantly higher than that of necrotic cells (Fig. [3]B, right), indicating that apoptosis rather than necrosis is the mechanism of 5-aza-CR-induced cell death in HCT-116 (+/+) cells. These findings collectively confirm that 5-aza-CR-induced increases in the sub-G_0-G_1 fraction (Fig. 2B) are due to apoptosis.

Inhibition of p53 Activation Abrogates 5-aza-CR-Induced Cell Cycle Arrest and Apoptosis. To assess the contribution of p53 activation in 5-aza-CR-induced growth inhibition, cell cycle arrest, and apoptosis, we employed the strategy of using PFT-α, a selective inhibitor of p53 function. The concentration of PFT-α that does not inhibit basal levels

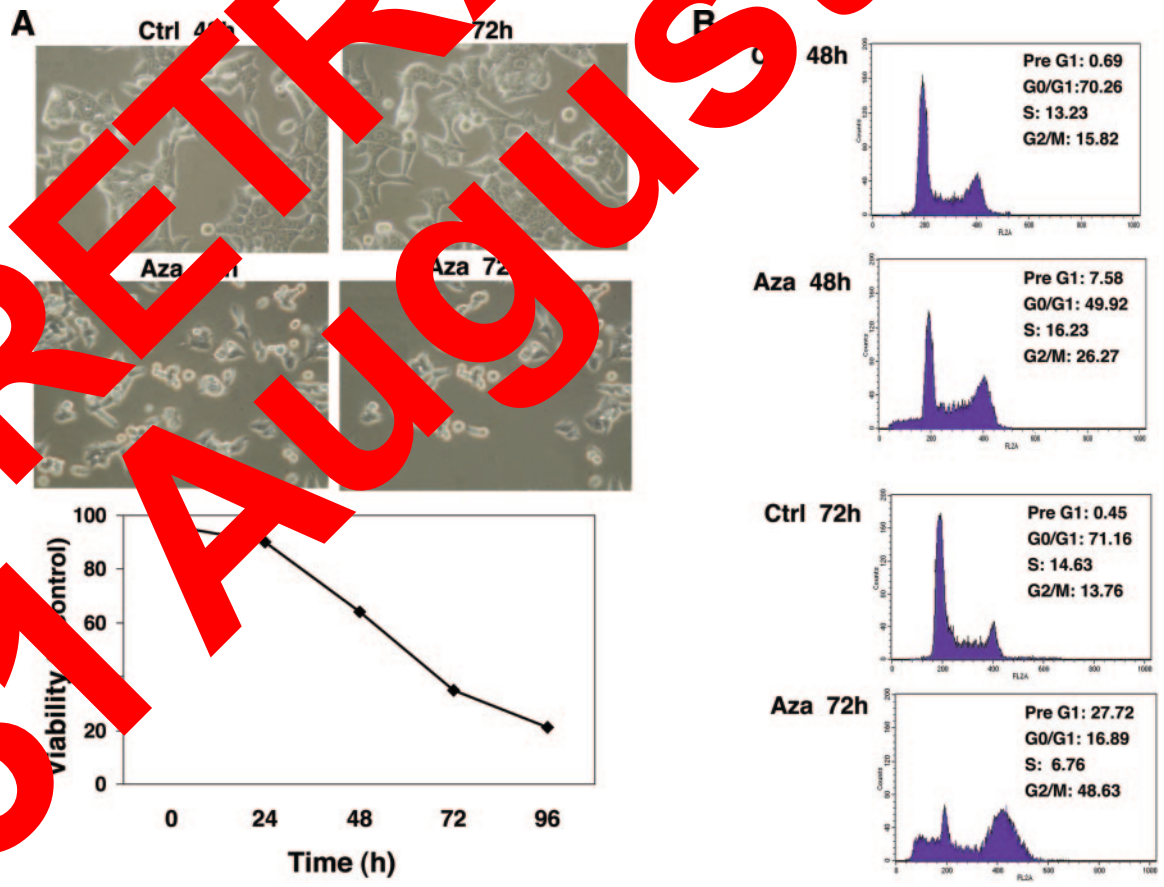

Fig. 2. Induction of growth/cell cycle arrest by 5-aza-CR in HCT-116 (+/+) human colon cancer cells. A, cell growth determined by the MTT assay. Controls were treated with ethanol. Values represent the means of duplicates from two separate experiments. B, effects on cell cycle profiles of HCT-116 cells after treatment with 1 μM 5-aza-CR. Cells in active growth were treated with 5-aza-CR for 48 or 72 h and then fixed, and the DNA content was determined by flow cytometric analysis by PI staining, analyzing 20,000 events per sample. The percentages of cells in PreG_1, G_0/G_1, S, and G_2/M are shown. The data shown are typical of one of three independent experiments.

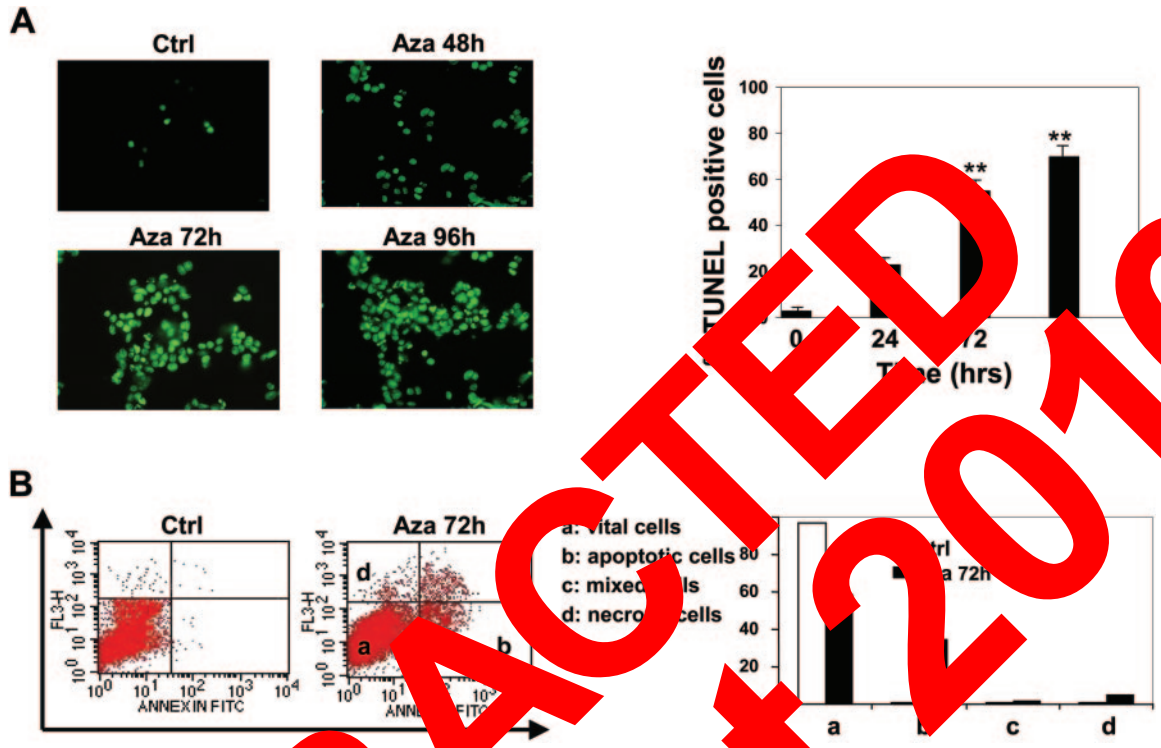

Fig. 3. The apoptotic effects of 5-aza-CR in HCT-116 (+/+) cells. A, cells treated with 5-aza-CR for 72 h, and the extent of DNA fragmentation determined by TUNEL assay in fixed and labeled cytospin preparations using fluorescence microscopy. The percentage of apoptotic cells also scored by the Annexin-V flow cytometric assay method, which can detect cells in an earlier stage of the apoptotic pathway and distinguish among apoptotic and necrotic cells.

of p53 protein expression. In control untreated cells and is not toxic to the cells when added at 30 μM. Seventy-two hours after addition of 5-aza-CR (1 μM), the percentage of viable cells increased from 24% in 5-aza-CR-treated cells to 80% cells treated with combination of 5-aza-CR and PFT-α (Fig. 4A). The fraction of cells in the G_1 phase increased 17% in 5-aza-CR treated cells, 58% in cells treated with a combination of 5-aza-CR and PFT-α, whereas the fraction of cells in the S phase decreased from 7 to 38% and 2% and The cell cycle kinetics of exponentially growing cells were altered by the addition of PFT-α (Fig. Furthermore, the number of apoptotic cells increased significantly to much higher levels than the untreated control when cultures were treated with a combination of 5-aza-CR and PFT-α (Fig. 4C). In agreement with these results the fraction of cells in G_1 phase decreased to 7%, and apoptosis was reduced in 5-aza-CR-treated p53 (−/−) cells (data not shown). These results demonstrate clearly that functional p53 is required for induction of apoptosis and cell cycle arrest in the G_2 phase by 5-aza-CR.

Several Apoptotic Genes Are Induced in Cells after Treatment with 5-aza-CR. We used GEArray Q series cDNA microarray to analyze expression changes of 96 key apoptotic genes in HCT-116 cells after treatment with 5-aza-CR. Cells were treated with 1 μM 5-aza-CR for 48 h, and their RNA was harvested for microarray analyses. A total of 5 genes (5.2%) was differentially expressed (>5-fold induction) after 5-aza-CR treatment. The up-regulated genes include RIPK2 (10-fold), Gadd45 (17-fold), BAK1 (16-fold), caspase 6 (20-fold), and caspase 5 (25-fold) (Table 2). These genes are associated with the regulation of either apoptosis (caspases, RIPK2, and BAK) or DNA damage (Gadd45) (Table 2). Real-time RT-PCR and Western blot analyses confirmed the induction of Gadd45 by 5-aza-CR treatment (Fig. 5, C and D).

5-aza-CR Treatment Results in Activation of p53 and Its Downstream Effectors $p21^{WAF1}$ and Gadd45. Growth arrest of cells by DNA damage and by other stress signals that arrest cells in G_2 is frequently associated with induction of Gadd45 (Taylor and Stark, 2001), and this was also found in HCT-116 (+/+) cells treated with 5-aza-CR (Fig. 5). Gadd45 can be induced by various mechanisms, including the p53 pathway, which is activated by phosphorylation on serine 15 in response to DNA damage and various other signals that induce G_2 cell cycle arrest (Taylor and Stark, 2001). Therefore we tested whether 5-aza-CR treatment resulted in an altered expression of p53. We observed a 2- to 5-fold induction of p53 protein expression in HCT-116 cells after 5-aza-CR treatment (Fig. 5A). Similar to Gadd45 and p53 activation, we observed a time-dependent increase of $p21^{WAF1}$ protein and transcript levels after 5-aza-CR treatment (Fig. 5, A and B). At 72 h post-treatment, a significant decrease in Bcl2 protein content to almost undetectable levels occurred in drug-treated cells (Fig. 5A), a time when apoptosis was extensive (Fig. 3). Despite the decrease in Bax protein expression, the Bax/Bcl2 ratio increased (48 h, 1.8-fold; 72 h, 2.4-fold) (Fig. 5A). Furthermore, treatment with 5-aza-CR resulted in a reduction in Bcl2 mRNA expression (Fig. 5C). Interestingly, when cells were allowed to recover from drug effects, the protein levels of p53, $p21^{WAF1}$, cyclin B1, Gadd45, and Bcl2 returned to levels of untreated control cells (Fig. 5A).

Role of p53 Activation in 5-aza-CR-Altered Protein Expression in HCT-116 Cells. To characterize the role of p53 in mediating 5-aza-CR-induced changes in protein ex-

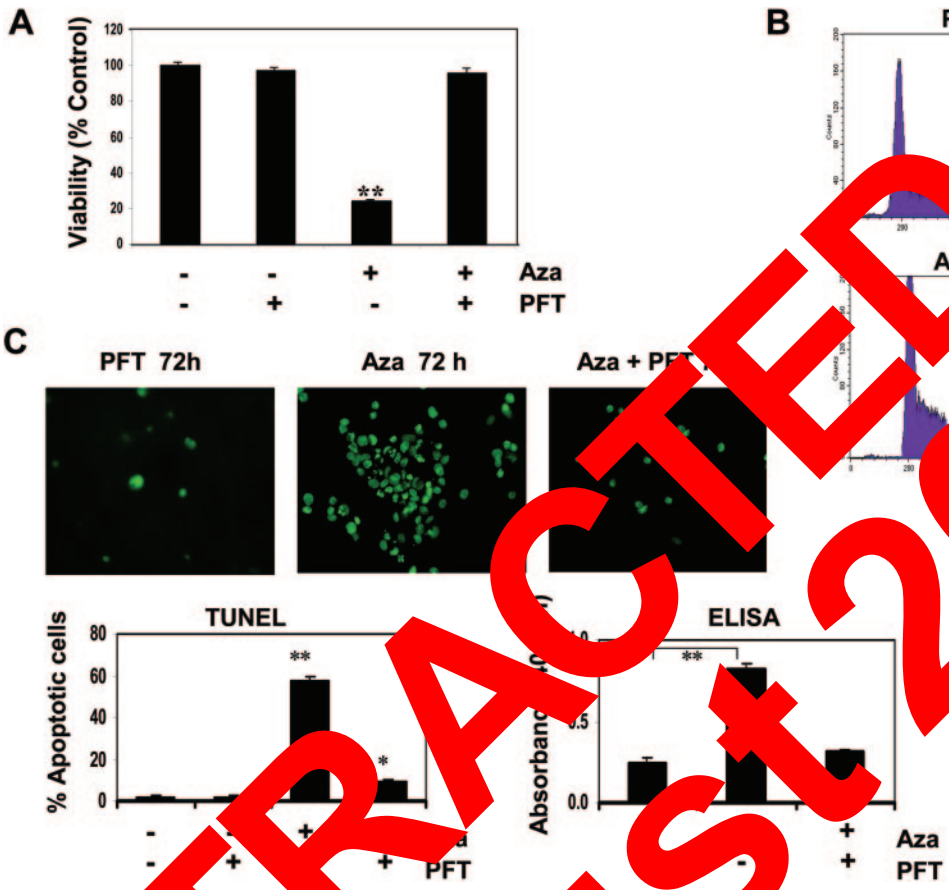

Fig. 4. Reversal of the g ibitory (A cycle (B), and apoptot effects a-CR by the p53 inhibitor PFT-α. HCT-116 cells were pretreated with 30 μM -α before tre ent with 1 μM 5-aza-C 72 h. cell growth determined by the MTT assay. B, DNA content determined by flow metric an following PI staining. Nu rical data esponding to cell cycle analysis are presented in boxes. C, DNA fragmentation det ned by TUNE ay in fixed and labeled in prep s using fluorescence microscopy.

TABLE 2

Profile of dys te nes after treatment of HCT-1 cells 5-aza-

The comp gene ne GEAr series Human Apop Gene Ar be found at http://www.superarray.com. All signals were measured using the Syngene BioIm em. n ge nes are indicated. Exp n ratios (sekeeping gene glyceraldehyde-3-phosphate dehydrogenase) were calculated per blot, and re re exp ld changes given as a rela ne exp cording to the formula ratio treatment/ratio control). Any signal whose raw intensity w ss than % of the ound was interpret be not the ple.

	Induction of Co	GenBa ccession No.	Potential Function
	%		
Dow ulated genes			
TRA	0.	NM005658	Tumor necrosis factor receptor-associated factor 1 Antiapoptotic
Up-regulated genes			
TNFRSF1B		NM001066	Proapoptotic
CASP14	0.64	NM012114	Unspecific in apoptosis
Casp	19.7	NM001226	Proapoptotic
Casp	25.0	NM004347	Proapoptotic
BLK	5.1	NM001715	Proapoptotic
BAK	15.5	NM001188	Proapoptotic
RIP	10.2	NM003821	Proapoptotic
ADD45	17.0	NM001924	Proapoptotic
K	4.1	HSU76376	Proapoptotic

[a] T ith 1 μM 5-aza-CR after 48 h.

press used PFT-α to investigate whether the abrogation of p53 induction in HCT-116 (+/+) cells treated with 5-aza-CR affects the level of expression of $p21^{WAF1}$, Bcl2, Bax, and Gadd45. Our results indicate that the induction of Gadd45 by 5-aza-CR treatment has a p53-dependent component because its expression was reduced by PFT-α (Fig. 5, A and D). For illustration, approximately a 5-fold induction of Gadd45 protein seen in 5-aza-CR-treated HCT-116 cells at 72 h disappeared when cells were exposed to the p53 inhibitor (Fig. 5A). A similar reduction in the magnitude of 5-aza-CR-induced Gadd45 mRNA expression was observed in HCT-116 cells treated with the inhibitor (Fig. 5D). On the other hand, PFT-α treatment did not significantly affect 5-aza-CR-induced $p21^{WAF1}$ transcript levels (Fig. 5B). Interestingly,

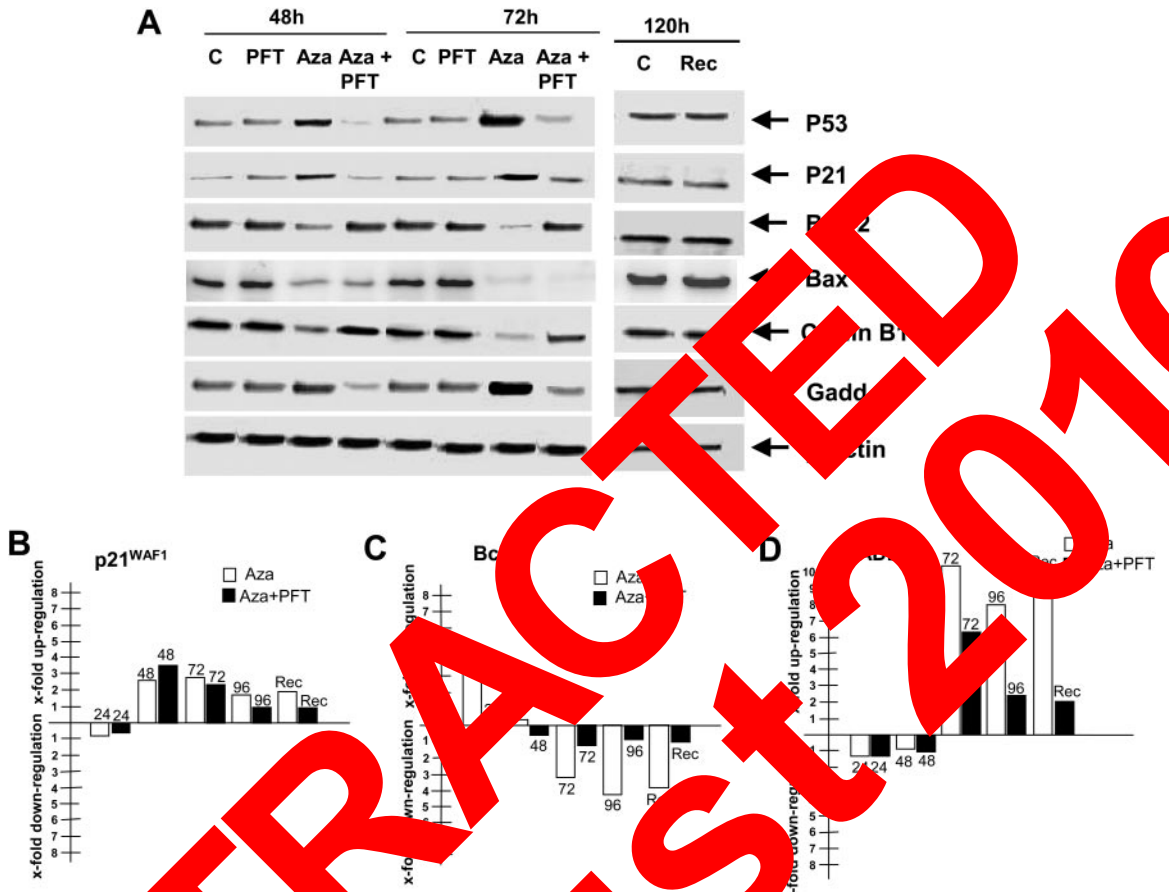

Fig. 5. A, Western blotti[ng] [a]nd[ly]s[is] the expres[sion] of Gadd45, p21^{WAF1}, p[53], cyclin B1, [and] BclII proteins in 5-aza-CR-treated (Aza), control (C), and PFT-α-treated (PFT) [HCT-116 p53 (+/+)] cells [were] treated with 30 μM PF[T] [for] 5 h prior to the addition of 1 μM 5-aza-CR. Total proteins were extracted, and the l[ysates] of protein [were] analyzed as described und[er] *Materials and Methods*. The blot was reprobed with an antibody directed against β-actin to confirm [equ]ivalent protein l[oad]ing. The immunoblots sho[wn] are repr[esentative] of the typical result from three independent experiments. B to D, effects of treat[ment] of cells with 5-aza-C[R] (Aza) and the p53 selectiv[e] inhibitor PFT-α (Aza + PFT) on the transcript levels of p21^{WAF1}, Bcl2, and Gadd45, respectively. Expression levels of mRNA were det[ermined] by qu[antitative] RT-PCR using a LightCycler. Relative mRNA values depicted are means ± S.D. [of] independent experiments, each p[erfor]med [in] duplicate. Rec, recovery; after 96 h, 5-aza-CR treatment was removed, and fresh medium [was] add[ed] to allow th[e cells] to recover from [the] effects [for] 72 h.

PF[T]-α rev[ersed] the [5]-aza-CR-elicited de[cr]ease [of] Gadd45 protei[n] expressio[n] (Fig. 5A) b[ut] not that of Bcl2 mRNA (Fig. 5C). I[n] co[ntrast], th[e] inhibitor experiment signifi[ed] that 5-aza[-CR] indu[ced] accumulation of Gadd45 [is] mediated [by] p53.

Reve[rsa]l of 5-aza-CR-Induced [Hy]pomethylation by the p53-Selective I[nhibitor] PFT-α. To investigate the role of p53 activation in 5-aza-CR-induced hypomethylation, we determined the effect [of] PFT-α on the DNA methylation status and on the expression of methyltransferases in drug-treated cells and studied the effect of 5-aza-CR on methyltransferase in HCT-116 cells lacking the p53 gene (Figs. 6 and 7). DNA isolated from HCT-116 (+/+) cells treated with the p53 inhibitor plus 5-aza-CR showed a greater degree of global genomic methylation compared with cells treated with the drug alone, suggesting that PFT-α prevented global DNA hypomethylation elicited by 5-aza-CR treatment (Fig. 6A). After cell recovery from 5-aza-CR exposure, the methylation-specific band generated by methylation-specific PCR appeared again (Fig. 6B). We then determined the effect of PFT-α on the expression of the human DNA methyltransferases DNMT1, DNMT3a, and DNMT3b in drug-treated HCT-116 cells. The inhibition of p53 activation restored the expression of DNMT3a protein (Fig. 6C) and the transcript levels of DNMT1 and DNMT3a (Fig. 6, D and E), suggesting that DNA demethylation by 5-aza-CR is related to p53 activity. DNMT1 mRNA expression was also down-regulated in 5-aza-CR-treated HCT-116 p53 (−/−) cells, in contrast to the DNMT3a mRNA expression level, which was not reduced. PFT-α treatment as well as the p53 knockout status of HCT-116 cells had no effect on DNMT3b mRNA expression (Figs. 6F and 7C). Although DNMT3a protein expression was greatly reduced in 5-aza-CR-treated HCT-116 (p53 +/+) cells, this protein did not completely disappear after 48 and 72 h of 5-aza-CR treatment in p53 −/− HCT-116 cells (Fig. 7D). This indicates a lack of p53 involvement and/or dissociation of DNMT3b response from DNMT1 and DNMT3a.

Discussion

In this study, we sought to elucidate the mechanism of 5-aza-cytidine-induced apoptosis, and, in addition, the possible link between demethylation and p53 induction in the p53 wild-type colorectal carcinoma cell line HCT-116. We observed that 5-aza-CR treatment arrests the cell cycle at G_2/M phase and induces apoptosis most likely by a joined activation of p53 protein and its downstream effectors GADD45 and p21^{WAF1}. This study investigates for the first time the expression of all three DNMTs in response to 5-aza-CR and

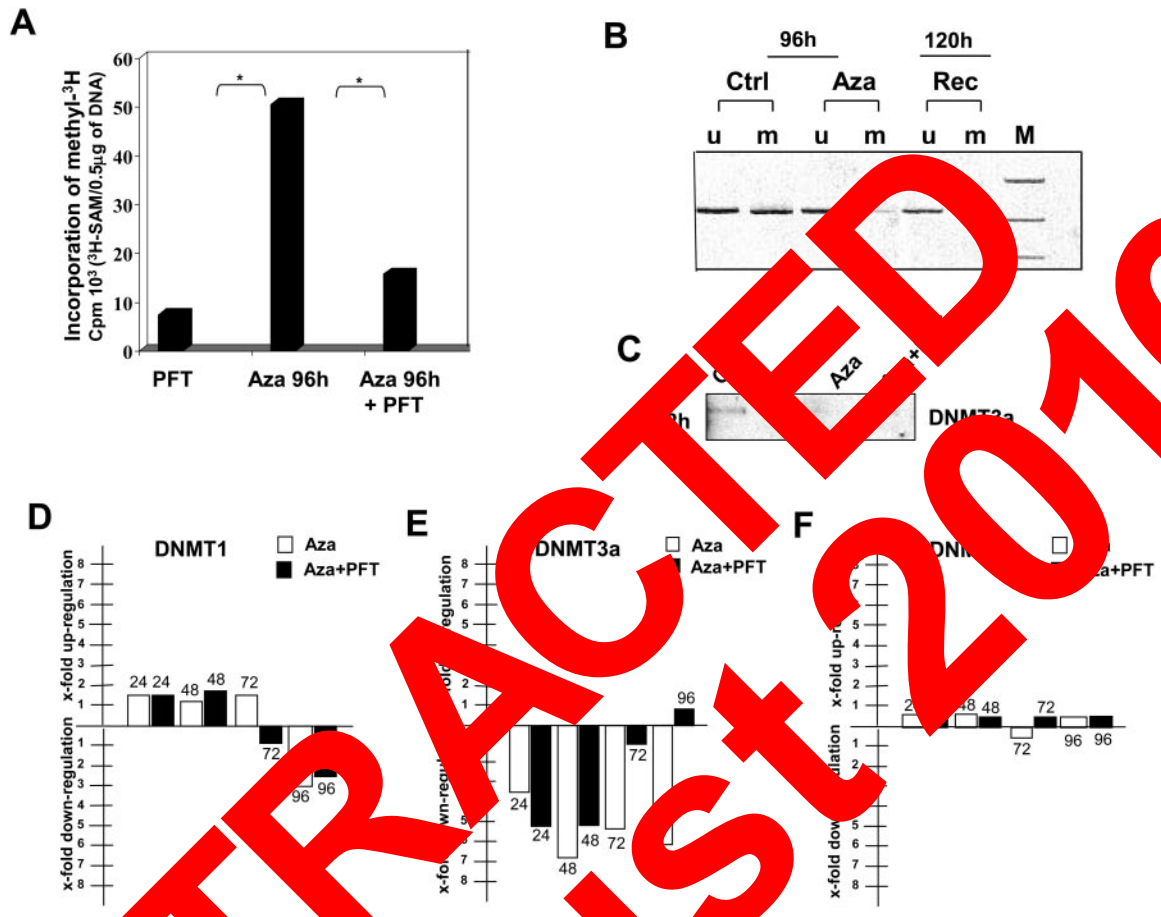

Fig. 6. Reversal of 5-aza-CR-induced hypomethylation by the p53-selective inhibitor PFT-α. A, effect of PFT-α on global DNA methylation status in 5-aza-CR-treated HCT-116 (+/+) cells. The extent of global DNA methylation is inversely proportional to the incorporation of methyl groups by SssI methylase in the presence of SAM. Values are means ± S.E.M., $n = 4$. ANOVA, Aza, 96 h, $p < 0.05$; Aza + PFT, 96 h, $p < 0.01$. B, effect of 5-aza-CR on $p16^{INK4a}$ promoter methylation. Methylation-specific PCR was performed using the unmethylated (u) and methylated (m) primer sets. C, effect of PFT-α on protein expression levels of the DNA methyltransferase DNMT1. D–F, effect on the transcript levels of DNMT1 (D), DNMT3a (E), and DNMT3b (F) in 5-aza-CR-treated HCT-116 cells.

its dependence on p53. We report further that 5-aza-CR caused a marked down-regulation of DNMT1 and DNMT3a mRNA levels in contrast to a null effect on DNMT3b. The down-regulation of DNMT1 resulted in global demethylation, which was confirmed by methylation-specific PCR showing reactivation of a silenced hemimethylated $p16^{INK4a}$ gene in cells. P53 dependence was confirmed by the finding that the DNA demethylation status was reversible upon treatment with the p53 inhibitor. The inhibition of p53 protein rendered HCT-116 cells less sensitive to 5-aza-CR-induced cell cycle- and apoptosis-related effects and restored the expression of GADD45, $p21^{WAF1}$, Bcl2, DNMT1, and DNMT3a proteins to normal untreated control. Furthermore, the absence of p53 function diminished the response of HCT-116 cells to the apoptotic and cell cycle modulatory effects of 5-aza-CR. P53 −/− cells showed no DNMT3a down-regulation (mRNA and protein levels) after 5-aza-CR-treatment, and DNMT1 and DNMT3b levels did not differ between p53 +/+ and p53 −/− cells. These methylation-dependent and -independent mechanisms are involved in 5-aza-CR action on HCT-116 cells.

For many years, 5-aza-CR has been used as a potent anticancer agent for the treatment of several hematopoietic neoplasms (Wijermans et al., 2000; Santini et al., 2001). However to date, the mechanisms of cellular responses of this drug are not well understood. Treatment with 5-aza-CR causes a variety of changes in cells, including decondensation of chromatin (Haaf and Schmidt, 1989), the activation of silenced genes and global genomic hypomethylation (Christman, 2002), and alterations in DNA replication timing (Jablonka et al., 1985), all of which are believed to be consequences of drug-induced demethylation. 5-aza-CR-induced cytotoxicity may be also related to enzyme adduct formation (Juttermann et al., 1994) whereby the incorporation of 5-aza-CR into DNA leads to the irreversible binding of DNMT1 to incorporated 5-aza-CR residues and the rapid loss of DNMT1 activity (Christman, 2002). To date, no studies have been conducted to investigate 5-aza-CR effects on the activity of DNMT3a and DNMT3b. These recently identified de novo methyltransferases are predicted to have the same response to this inhibitor as DNMT1, yet this has not been proven. There is reason to suspect that DNMT3a and DNMT3b respond much more to the inhibitory effects of 5-aza-CR residues incorporated into DNA since they are randomly incorporated in place of cytidine, and, unlike DNMT1, DNMT3a and DNMT3b are capable of methylating cytidine residues that are not in CpG islands (Aoki et al., 2001). The p53 dependency of the DNMT3a expression, but not that of DNMT3b, is surprising when considering the fact that both enzymes are de novo methyltransferases. It is noteworthy to mention that mice embryos lacking both copies of DNMT3b

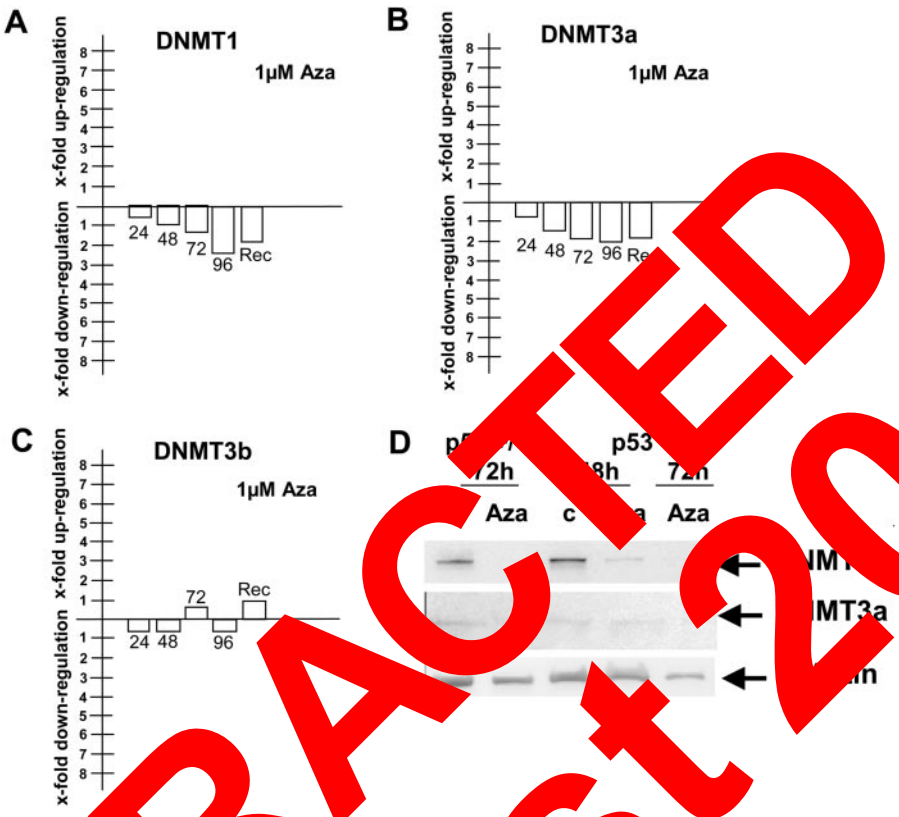

Fig. 7. A to D, time-course analysis of mRNA (A–C) and protein expression of the DNA methyltransferases DNMT1, DNMT3a, and DNMT3b in HCT-116 (−/−) cells after exposure of 1 μM 5-aza-CR.

die before birth, whereas DNMT3a-null mice survive for about 4 weeks (Okano et al., 1999). DNMT3b targets specially centromeric satellite repeats and is linked to lymphocyte-mediated immunological defects (Hansen et al., 1999). In addition, DNMT1 and DNMT3b have overlapping functions in global methylation during early embryogenesis (Reik, 1999). However, the enzymes may have distinct or tissue-specific functions during later embryogenesis, tumorigenesis (Bestor, 2000). In this respect, in further studies it will be of interest if the observed effect of DNMT3a expression is specific for colon cancer cell lines. However, the mechanism by which p53 regulates DNMT3a expression is still unknown.

p53 has been shown to be critical in growth arrest and apoptosis in response to DNA damage by chemotherapeutic agents (Lakin and Jackson, 1999). The p53 status has a significant impact on the cancer cell sensitivity to 5-aza-CR (Karpf et al., 2001, 2004). The role of p53 in the apoptotic efficacy of 5-aza-CR is controversial. In some systems (HCT-116), the presence of wild-type p53 is essential for apoptosis induction, whereas in other systems (mouse embryonic fibroblasts), the absence of p53 determines a higher chemotherapeutic index for 5-aza-CR (Karpf et al., 2001; Nieto et al., 2004). Wild-type p53 colon cancer cells were more sensitive to 5-aza-CR-mediated growth arrest and cytotoxicity, whereas cells expressing mutant p53 protein were not affected by 5-aza-CR (Karpf et al., 2001; Nieto et al., 2004). In agreement with the latter studies, we show an induction of p53 protein and a significant decrease in the antiapoptotic Bcl2 protein in response to 5-aza-CR. p53 protein expression increased about 4-fold, whereas Bcl2 protein expression was almost undetectable after 72 h, an incubation period when apoptosis was massively induced. This supports other reports demonstrating that the overexpression of Bcl2 protein inhibits p53-mediated apoptosis and p53-mediated transcriptional activation (Shen and White, 2001). After drug recovery, p53 protein expression declined to control levels. Upon treatment with PFT-α or in p53 −/− cells, apoptosis induction was markedly reduced, indicating that p53 is a major modulator of 5-aza-CR-induced apoptosis. Our findings are in agreement with the hypothesis that 5Aza-CR induces DNA damage post-translationally by stabilizing the p53 protein (Lakin and Jackson, 1999). Normally, p53 protein has a relatively short half-life, being rapidly targeted for ubiquitination and degradation. Following cellular stress, the p53 protein is phosphorylated, increasing its half-life and transactivation activity (Meek, 1994). In our study, the increase in p53 protein expression does not appear to be transcriptionally induced as measured by real-time RT-PCR. This finding is in accordance with that reported by Karpf et al. (2001) using northern blotting analysis. Thus, we cannot suggest a possible demethylation of the p53 promotor by 5-aza-CR.

To further understand the mechanism of 5-aza-CR-mediated p53 activation, we investigated the DNA damage-inducible gene, GADD45 (Wang et al., 1999). It is known that p53 is a transcriptional activator of GADD45 (Wang et al., 1999). Nevertheless, the mechanisms for p53 dependence of the GADD45-induced cell cycle G_2/M arrest are not clear at the present time (Jin et al., 2002). Earlier studies have shown that the microinjection of a GADD45 expression vector into normal fibroblasts resulted in G_2/M arrest, which could be attenuated by cyclin B1 overexpression (Wang et al., 1999). In our study, a dose-dependent accumulation of cells in G_2/M

after 5-aza-CR treatment was indeed confirmed by down-regulation of cyclin B1 expression. We also demonstrate that 5-aza-CR treatment remarkably up-regulated GADD45 expression by an intracellular pathway via p53 induction. Recovering from 5-aza-CR treatment as well as PFT-α treatment restored the GADD45 protein levels to untreated controls and inhibited GADD45 mRNA expression. However, the induction in the transcript level of GADD45 upon 5-aza-CR treatment did not change upon recovery. This discrepancy suggests that both transcriptional and post-transcriptional mechanisms contribute to the GADD45 expression after 5-aza-CR treatment. p53-dependent and -independent mechanisms have been reported to play a role in the regulation of GADD45 expression (Lakin and Jackson, 1999). In addition, the pathway down stream from GADD45 observed in 5-aza-CR-treated cells remains to be elucidated.

The up-regulation of $p21^{WAF1}$ is believed to be a ma... mediator of p53-dependent G_1 arrest, causes cells to acc...d-late in both G_1 and G_2 after DNA damage, and is asso...ted with a reduction of cyclin B1 expression (Medema ...al., 1998; Jin et al., 2002). We determined whet...er $p21^{W...}$ required for GADD45-mediated G_2/M arrest, ...$21^{W...}$ binding to GADD45 in vivo has been previous...locu... (Chen et al., 1995). We show that initiation of ...A d...age by 5-aza-CR is accompanied by a tim...endent ...tion of $p21^{WAF1}$ protein.

Furthermore, $p21^{WAF1}$ and ...in B1 ...rotein e...ression were inversely correlated u...g t...brogation of p53 after PFT-α redu...p21 ...protein expression to untreated control level... did not ... the mRNA expression level. Thus, p2...duction a... 5-aza-CR has a p53-dependent co...onent an...n be modulated on the ...n-scriptional lev... Such uncoup...of $p21^{WAF1}$ mRNA ... protein exp...ion w...found to occur in severa... lin... upon expos...to ...notoxic stress (Butz et a... The induct...of p2...1 prot...has been shown ...er treat...t of t...lls ...h ...isense oligonucle...s dir... a...nst D...MT1 (...el et al., 199... oli...ide ...d s...inhibitors of DNMT1 ...utinovic et al. 20... inhibition ... DNMT1 can i...uce p21 ... prot...-els by ...ost-translational mecha...as re...y suggested by Fou...et al. (19...Recent st...d...monstrated the ability of $p21^{WAF1}$ to ...GAD...5 (Kearsey et al., 1995) as well as DN...1 co...for association with proliferating cell nuclea...n (Chuang et al., 1997). Further exp...iments are req...d to clarify this association.

In con...on, this study ...monstrates that 5-aza-CR inhibits D... and DNMT... activity in HCT-116 colorectal cancer c...s a...uses CpG demethylation and reactivation ...hylation-si...d genes. To our knowledge, this is the first ...monstration ...f p53-dependent 5-aza-CR action on de nov... ...transferase DNMT3a. The effects on apoptosis and cell cy... arrest, as well the inhibitory effects on cell growth i...ated by 5-aza-CR in HCT-116 cells are caused by methy...ion-dependent and independent pathways.

Acknowledgments

We thank Simone Staeck, Uta Schoenborn, and Antje Schinlauer for excellent technical assistance.

References

Aoki A, Suetake I, Miyagawa J, Fujio T, Chijiwa T, Sasaki H, and Tajima S (2001) Enzymatic properties of de novo-type mouse DNA (cytosine-5)-methyltransferases. *Nucleic Acids Res* **29:**3506–3512.

Bestor TH (2000) The DNA methyltransferases of mammals. *Hum Mol Genet* **9:**2395–2402.

Bird AP (1996) The relationship of DNA methylation to cancer. *Cancer Surv* **28:**87–101.

Butz K, Geisen C, Ullmann A, Ze... Hoppe-Seyler F (1998) Uncoupling of p21WAF1/CIP1/SDI1 mRN... prote...ssion upon genotoxic stress. *Oncogene* **17:**781–787.

Chen IT, Smith ML, O'Co... M, and Forna... J Jr (1995) Di...action of Gadd45 with PCNA ...nd ...ce for comp...ve interacti... Gadd45 and p21Waf1/Cip1 wit...NA. *O...e* **11:**193...37.

Christman JK (20...-azacytidine ...5-aza-...eoxycytidine as ...bi... of ... methylation: ...hanistic ...dies ... ...mplicatio... for ca... ...apy. *Oncogene* **21:**...5495.

Chuang L... L. J... TW, Ng HH, Xu G, and Li... 997) I... DNA (cyto...) m...sferase-P... complex target f...2 ...1. *Sci... DC...*:1996–2...

Fo... M, Sapieha ...ali..., Besterm... and ...acLeod... 999) Down-... of human ...osine-5) ...rase induces ...cle regu-lators ...k4A) and ...WAF1/Cip...a dis...echanisms. *...ol Chem* **274:**242...256.

Ali-Muhtas... Diab-Assaf M, Boltze C... Hmaira J... ...sner A, Hartig R, and Schneider-St... (2004) Thy...inone ...es apop...in human colorectal cancer HCT-116 ...lls throu...epen...echani... *Int J Oncol* **25:**857–866.

Haaf ... Schmidt M (198... Azaded...tidine i... ...der condensation in the giar... chromosomes of ...*tus ag...s*. *Chromosoma* **98:**93–98.

Hans... S, Wijmenga C, ...do P, St... AM, ...anfield TK, Weemaes CM, and ... SM (1999) The DNMT3B D... meth...sferase gene is mutated in the ... immunodeficiency syndrome. *P... ...d Sci USA* **96:**14412–14417.

Jablonka E, Go...in R, Marcus M, and ... (1985) DNA hypomethylation causes an increase i... sensitivity an... dvance in the time of replication of the entire inactive... ...osome. *Chromos...a* **93:**152–156.

Jin S, Tong T, ...Fan F, Antinore MJ, Zhu X, Mazzacurati L, Petrik KL, Rajasekaran B, W... et al. (2002) GADD45-induced cell cycle G2-M arrest associat...h altera... ...lar distribution of cyclin B1 and is dependent of p38 ... activity. *Onc...* **1:**8696–9704.

Jutte... ...nn R, ... and Jaenisch R (1994) Toxicity of 5-aza-2′-deoxycytidine to m... ...mediated primarily by covalent trapping of DNA methyltra... ...ath... ...han DNA demethylation. *Proc Natl Acad Sci USA* **91:**1179...1801.

...rpf AR, I... ..., Ririe TO, Hanks AN, Grossman D, and Jones DA (2004) ...ited g... ...ivation in tumor and normal epithelial cells treated with the DNA ...ltransferase inhibitor 5-aza-2′-deoxycytidine. *Mol Pharmacol* **65:**18–27.

Kar... Moore BC, Ririe TO, and Jones DA (2001) Activation of the p53 DNA da... response pathway after inhibition of DNA methyltransferase by 5-aza-2′-de...cytidine. *Mol Pharmacol* **59:**751–757.

...ey JM, Coates PJ, Prescott AR, Warbrick E, and Hall PA (1995) Gadd45 is a ...clear cell cycle regulated protein which interacts with p21Cip1. *Oncogene* **11:**1675–1683.

Kho PS, Wang Z, Zhuang L, Li Y, Chew JL, Ng HH, Liu ET, and Yu Q (2004) p53-regulated transcriptional program associated with genotoxic stress-induced apoptosis. *J Biol Chem* **479:**21183–21192.

Kitagawa Y, Kyo S, Takakura M, Kanaya T, Koshida K, Namiki M, and Inoue M (2000) Demethylating reagent 5-azacytidine inhibits teloemerase activity in human prostate cancer cells through transcriptional repression of hTERT. *Clin Cancer Res* **6:**2868–2875.

Kornblith AB, Herndon JE 2nd, Silverman LR, Demakos EP, Odchimar-Reissig R, Holland JF, Powell BL, DeCastro C, Ellerton J, Larson RA, et al. (2002) Impact of azacytidine on the quality of life of patients with myelodysplastic syndrome treated in a randomized phase III: a cancer and leukemia group study. *J Clin Oncol* **20:**2441–2452.

Lakin ND and Jackson SP (1999) Regulation of p53 in response to DNA damage. *Oncogene* **18:**7644–7655.

Medema RH, Klompmaker R, Smits VA, and Rijksen G (1998) p21waf1 can block cells at two points in the cell cycle, but does interfere with processive DNA-replication or stress-activated kinases. *Oncogene* **16:**431–441.

Meek DW (1994) Post-translational modification of p53. *Semin Cancer Biol* **5:**203–210.

Milutinovic S, Knox JD, and Szyf M (2000) DNA methyltransferase inhibition induces the transcription of tumor suppressor p21(WAF1/CIP1/sdi1). *J Biol Chem* **275:**6353–6359.

Nieto M, Samper E, Fraga MF, de Buitrago GG, Esteller M, and Serrano M (2004) The absence of p53 is critical for the induction of apoptosis by 5-aza-2′-deoxycytidine. *Oncogene* **23:**735–743.

Okano M, Bell DW, Haber DA, and Li E (1999) DNA methyltransferases Dnmt3a and Dnmt3b are essential for de novo methylation and mammalian development. *Cell* **99:**247–257.

Petti MC, Mandelli F, Zagonel V, De Gregoris C, Merola MC, Latagne R, Gattei V, Fazi P, Monfardini S, and Pinto A (1993) Pilot study of 5-aza-2′-deoxycytidine (Decitabine) in the treatment of poor prognosis acute myelogenous leukemia patients: preliminary results. *Leukemia Suppl* **1:**36–41.

Reik W, Kelsey G, and Walter J (1999) Dissecting de novo methylation. *Nat Genet* **23:**380–382.

Saha S, Bardelli A, Buckhaults P, Velculescu VE, Rago C, Croix B, Romans KE, Choti MA, Lengauer C, Kinzler KE, et al. (2001) A phosphatase associated with metastasis of colorectal cancer. *Science (Wash DC)* **294:**1343–1346.

Santini V, Kantarjian HM, and Issa JP (2001) Changes in DNA methylation in neoplasia: pathophysiology and therapeutic implications. *Ann Intern Med* **134:** 573–586.
Schneider-Stock R, Boltze C, Lasota J, Miettinen M, Peters B, Pross M, Roessner A, and Günther T (2003) High prognostic value of $p16^{INK4}$ alterations in gastrointestinal stromal tumors. *J Clin Oncol* **9:**1688–1697.
Shen Y and White E (2001) p53 dependent apoptotic pathways. *Adv Cancer Res* **82:**55–84.
Silverman LR, Demakos EP, Peterson BL, Kornblith AB, Holland JC, Odchimar-Reissig R, Stone RM, Nelson D, Powell BL, DeCastro CM, et al. (2002) Randomized controlled trial of azacytidine in patients with the myelodysplastic syndrome: a study of the cancer and leukemia group B. *J Clin Oncol* **20:**2429–2440.
Taylor WR and Stark GR (2001) Regulation of the G2/M transition by p53. *Oncogene* **20:**1803–1815.
Wang A, Yoshimi N, Ino N, Tanaka T, and Mori H (1997) Overexpression of cyclin B1 in human colorectal cancers. *J Cancer Res Clin Oncol* **123:**124–127.
Wang XW, Zhan Q, Coursen JD, Khan MA, Kontny HU, Yu L, Hollander MC, O'Connor PM, Fornace AJ Jr, and Harris CC (1999) GADD45 induction of a G2/M cell cycle checkpoint. *Proc Natl Acad Sci USA* **96:**3706–3711.
Wijermans P, Lubbert M, Verhoef G, Bosly A, Ravoet C, Andre M, and Ferrant A (2000) Low-dose-5-aza-2′-deoxycytidine, a DNA hypomethylating agent for the treatment of high-risk myelodysplastic syndrome: a multicenter phase II study in elderly patients. *J Clin Oncol* **18:**956–962.
Zhu WG and Otterson GA (2003) The interaction of histone deacetylase inhibitors and DNA methyltransferase in[illegible] the treatment of human cancer cells. *Curr Med Chem Anti-Cancer* [illegible]9.

Address correspondence to: Dr. Regine[illegible]neider-Stock[illegible]ment of Pathology, Division [illegible]lecu[illegible]enetics, Ott[illegible]n-Guericke[illegible]versity, Leipziger Str. 44, 3912[illegible]agdebu[illegible]ermany. E-mail: regine.[illegible]neide[illegible]@medizin.uni-ma[illegible]burg.de

Correction to “5-aza-Cytidine Is a Potent Inhibitor of DNA Methyltransferase 3a and Induces Apoptosis in HCT-116 Colon Cancer Cells via Gadd45- and p53-Dependent Mechanisms”

In the above article [Schneider-Stock R, Diab-Assef M, Rohrbeck A, Foltzer-Jourdainne C, Boltze C, Hartig R, Schonfeld P, Roessner A, and Gali-Muhtasib H (2005) *J Pharmacol Exp Ther* **312**:525–536], similar groups of cells appear at different time points in Figures 2A and 3A that have raised suspicion regarding the original preparation of these figures. Given the length of time since original publication, the exact reason for this discrepancy could not be determined. These experiments have been repeated and the new data clearly support the main message of the manuscript on the pro-apoptotic effects of 5-aza-cytidine (5-aza-CR).

Corrected figure panels are reprinted below with new legends. A *Methods* for the repeated experiments is also provided.

The authors regret this error and any inconvenience it may have caused.

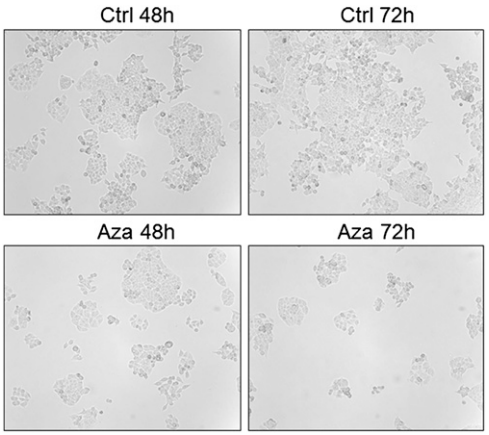

Fig. 2A. Induction of growth arrest by 5-aza-CR (Aza) in HCT-116 (+/+) human colon cancer cells. Cell were seeded and treated with 1 μM 5-aza-CR for 48 and 72 hours. Representative bright field images were taken of two separate experiments. Ctrl, control.

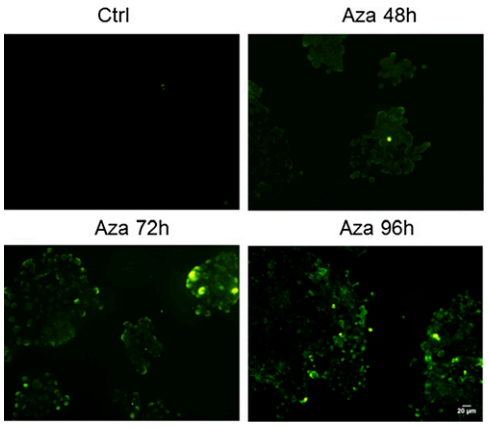

Fig. 3A. The apoptotic effects of 5-aza-CR (Aza) in HCT-116 (+/+) cells. Cells treated for 48, 72, and 96 hours with 1 μM 5-aza-CR and the extent of DNA fragmentation determined by TUNEL assay (green) in fixed cells using fluorescence microscopy. Bar, 20μm; Ctrl, control.

Methods

Cell Growth and Treatment. The human colon cancer HCT-116 cells were cultured in RPMI 1640 medium. Cells were grown at 37°C in an atmosphere of 5% CO2 supplemented with penicillin (100 U/ml), streptomycin (100 mg/ml), and 10% fetal calf serum. For experiments, cells were seeded on six-well plates at a density of 40,000 cells per well. Cells were treated with 1 μM of freshly prepared 5-aza-CR (Sigma-Aldrich, St. Louis, MO) 24 hours after plating, and treatment was replenished every 48 hours. Randomly selected bright field microscopic fields were acquired on an inverted microscope Leica DMi1 (Wetzlar, Germany) using 4× and 10× air objective lenses.

Apoptosis: Terminal Deoxyribonucleotidyl Transferase–Mediated dUTP Nick-End Labeling Assay. Apoptosis was scored by estimating the extent of DNA fragmentation using the terminal deoxyribonucleotidyl transferase–mediated dUTP nick-end labeling (TUNEL) assay. Briefly, cells were plated on autoclaved glass coverslips in six-well culture plates and treated with 1 μM 5-aza-CR. The medium was then aspirated and cells were washed twice with warm phosphate-buffered saline. Cellular DNA was stained with the In Situ Cell Death Detection kit (Roche Diagnostics, Mannheim, Germany), and the assay was performed according to the recommendations of the manufacturer. For each of three replicated experiments four randomly selected microscopic fields were acquired on an inverted microscope Nikon eclipse Ti-U (Tokyo, Japan) using a 20× air objective lens (Nikon). The same microscopy setup was used for all representative images. Bar, 20μm.